ACS APPLIED MATERIALS & INTERFACES

Research Article

www.acsami.org

Engineered Nanotopography on Electrospun PLLA Microfibers Modifies RAW 264.7 Cell Response

Nicholas J. Schaub,[†,‡] Tara Britton,[†,‡] Rupak Rajachar,[§] and Ryan J. Gilbert*[,†,‡]

[†]Center for Biotechnology and Interdisciplinary Studies, Rensselaer Polytechnic Institute, Troy, New York 12180-3590, United States

[‡]Department of Biomedical Engineering, Rensselaer Polytechnic Institute, Troy, New York 12180-3590, United States

[§]Department of Biomedical Engineering, Michigan Technological University, Houghton, Michigan 49931-1295, United States

Supporting Information

ABSTRACT: In this study, we created a new method of electrospinning capable of controlling the surface structure of individual fibers (fiber nanotopography). The nanotopographical features were created by a phase separation in the fibers as they formed. To control the phase separation, a nonsolvent (a chemical insoluble with the polymer) was added to an electrospinning solution containing poly-L-lactic acid (PLLA) and chloroform. The nanotopography of electrospun fibers in the PLLA/chloroform solution was smooth. However, adding a small weight (<2% of total solution) of a single nonsolvent (water, ethanol, or dimethyl sulfoxide) generated nanoscale depressions on the surface of the fibers unique to the nonsolvent added. Additionally, nanoscale depressions on electrospun fibers were observed to change with dimethyl sulfoxide (DMSO) concentration in the PLLA/chloroform solution. A nonlinear relationship was found between the concentration of DMSO and the number and size of nanotopographical features. The surface depressions did not alter the hydrophobicity of the scaffold or degradation of the scaffold over a two-day period. To determine if fiber nanotopography altered cell behavior, macrophages (RAW 264.7 cells) were cultured on fibers with a smooth nanotopography or fibers with nanoscale depressions. RAW 264.7 cells spread less on fibers with nanoscale depressions than fibers with a smooth topography ($p < 0.05$), but there were no differences between groups with regard to cell metabolism or the number of adherent cells. The results of this study demonstrate the necessity to consider the nanotopography of individual fibers as these features may affect cellular behavior. More importantly, we demonstrate a versatile method of controlling electrospun fiber nanotopography.

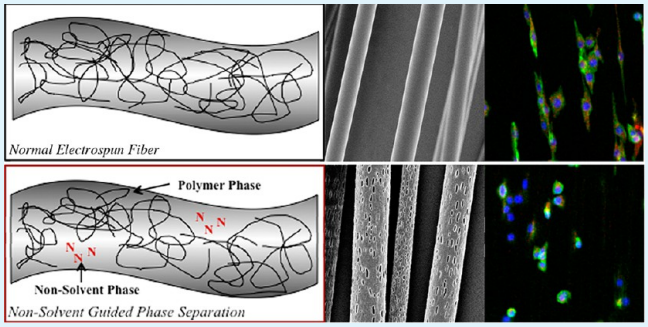

KEYWORDS: *electrospun fibers, phase separation, topography, PLLA, RAW 264.7 cells*

1. INTRODUCTION

Electrospinning generates polymeric fibers with diameters ranging from tens of nanometers to several micrometers.[1] Additionally, physical characteristics of the fibers are tunable to create scaffolds with highly aligned fibers and individual fibers of varying diameter. The rationale for creating electrospun fiber scaffolds of varying physical characteristics is that the cell response is altered by the presence of particular fiber characteristics.[2,3] Studies evaluating cellular response to electrospun fibers frequently assess the influence of fiber alignment and diameter on cell behavior. Electrospun fibers are randomly oriented if collected on a grounded plate due to the intense electrostatic forces that cause a whipping action of the polymer-solvent jet,[4,5] but the fibers may be aligned if collected on a rotated disk[6,7] or using two grounded plates separated by a gap.[8,9] By varying fiber alignment, electrospun fiber scaffolds can mitigate cellular migration so that aligned fibers support directed migration along the fibers verse randomly oriented fiber substrates that enable cellular migration in all directions. Fiber alignment is known to influence the direction and extent of neurite extension,[6,10−20] and the directed migration of fibroblasts,[21] gliomas,[22] and ligament cells.[23] Additionally, fiber alignment is known to alter fibrous tissue formation in vivo[24] and inflammatory markers of macrophages in vitro.[25] Electrospun fiber diameter is also easily modified by changing the concentration of polymer in the electrospinning solution,[26,27] polymer molecular weight,[28] relative humidity,[29] and even solution temperature.[30]

Fibers with diameters on the nano to micro scale are of interest as cell adhesion scaffolds since electrospun fibers with these diameters are believed to mimic fibrous structures in the native extracellular matrix. Electrospun fiber diameter in particular is known to regulate cell behavior. As an example, a recent study by Lee et al. demonstrated that oligodendrocytes myelinate electrospun polystyrene fibers only when the fibers possessed diameters larger than 4 μm.[31] This study suggests

Received: July 17, 2013
Accepted: September 24, 2013
Published: September 24, 2013

that fiber diameter can trigger a desired cell response in the absence of chemical or biological cues. More generally, a wide variety of cell types show a significantly different response when cultured on electrospun fibers with submicrometer diameters (less than 750 nm) compared to fibers with diameters larger than one micrometer. Changes in cell behavior when cultured on submicrometer fibers compared to fibers larger than a micrometer include changes in neurite guidance,[32−36] changes in cell migration of fibroblasts[21] and osteoblasts,[37] osteoblast differentiation and proliferation,[38] macrophage cytokine production,[25] and even neural stem cell differentiation.[39] Indeed, careful control of electrospun fiber diameter is important in engineering the cellular response to these materials.

Since nanoscale fiber diameter is known to alter cell behavior, it is reasonable to propose that fiber nanotopography may also regulate cell function. Fiber nanotopography (i.e. the nanoscale surface structure of individual fibers) is known to change with the polymer-solvent mixture used to electrospin fibers or when the relative humidity of the electrospinning environment is changed.[40−42] Many cell studies use fibers without characterizing fiber nanotopography. In fact, only a few studies have investigated the effects of fiber nanotopography on cellular behavior. Leong et al. reported an increase in protein adsorption and epithelial cell viability on electrospun poly(D,L-lactide) scaffolds with a rough fiber surface compared to electrospun scaffolds with a smooth fiber surface.[43] Furthermore, Moroni et al. generated terephthalate composite fibers using different polymer-solvent mixtures and evaluated human mesenchymal stem cells (hMSCs) response on fibers with smooth or rough fiber surfaces.[44] hMSCs were more proliferative on electrospun fibers with a rough nanotopography compared to electrospun fibers with a smooth nanotopography. The study by Moroni et al. is unique among the few papers investigating cells on electrospun fibers with different nanotopographies because the fiber diameter was the same between fiber groups with different nanotopography. By ensuring fiber scaffolds had similar fiber diameter between groups with different nanotopography, Moroni and colleagues were able to decouple the effect of fiber diameter from fiber nanotopography, effectively demonstrating how cell behavior is altered by the surface structure of individual fibers apart from fiber diameter. The results of the Moroni study suggest that electrospun fiber nanotopography may be a new topic of interest in directing cell behavior in addition to other features of the electrospun scaffolds, such as fiber diameter.

To facilitate investigations involving electrospun fiber nanotopography, one goal of this study was to develop a new procedure to place defined nanotopography onto the surface of electrospun fibers. We hypothesized that nanotopography could be engineered using a standard electrospinning solution containing a polymer, an organic solvent, and a nonsolvent. The nonsolvent would be immiscible with the polymer but soluble with the organic solvent creating a phase separation in the fiber as it is formed during electrospinning. If different nonsolvents interact with the polymer/solvent mixture differently, a fiber topography unique to each nonsolvent should be generated upon electrospinning, making the method highly versatile.

To test the hypothesis, a nonsolvent (water, ethanol, or DMSO) was added to a solution containing poly-L-lactic acid (PLLA) dissolved in chloroform. Electrospinning the PLLA and chloroform solution without a nonsolvent resulted in electrospun fibers with a smooth surface. Electrospinning solutions containing a nonsolvent created fibers with unique nanotopographies consisting of depressions in the surface of the fiber. To determine if the concentration of nonsolvent altered fiber nanotopography, increasing concentrations of DMSO were added to PLLA/chloroform solutions. As DMSO concentration increased in the electrospinning solution, the resultant fibers revealed changes in the size and number of nanotopographical depressions. To determine if the presence of nanoscale depressions altered cell behavior, RAW 264.7 cells were cultured on fibers with and without nanoscale depressions. Cell elongation, adhesion, and metabolic activity were assessed on the different electrospun fiber scaffolds. Unlike the hMSC study where hMSCs elongated more on fibers with a rough nanotopography,[13] RAW 264.7 cells elongated less on fibers with nanoscale depressions. The reduction in cell elongation was not accompanied by any significant differences in the number of adherent cells or a change in cell metabolism. The data from the RAW 264.7 cell experiments provides evidence that the topography of individual electrospun fibers is capable of altering cell behavior. As electrospun fibrous scaffolds continue to emerge as tissue engineering scaffolds, procedures that can finely control the shape and prominence of nanotopographical features may aid in the control of cell behavior to facilitate robust tissue repair.

2. MATERIALS & METHODS

2.1. Electrospinning. *2.1.1. Preparation of Electrospun Fibers without Nanotopography.* Poly-L-lactic acid (PLLA, NatureWorks; grade 6201D, Lot #9051-89-2) was purchased from Cargill Dow LLC (Minnetonka, MN). 1,1,1,6,6,6-hexafluoro-2-propanol (HFP), chloroform, and dimethyl sulfoxide (DMSO) were purchased from Sigma (St. Louis, MO).

The electrospinning device utilized here was previously described.[6,32,45] A PLLA film was air cast onto 15 mm square glass coverslips using a solution containing 3 g each of chloroform and dichloromethane with 240 mg of PLLA. All solutions were electrospun using the following conditions: relative humidity <28%, temperature 21−23°C, 1000 rpm collecting disc rotation speed, 15 kV drawing voltage, 5.5 cm needle to collection distance, 2 mL/h syringe pump flow rate, and 20 min collection time.

2.1.2. Preparation of Electrospun Fibers with Nanotopography. All electrospinning solutions used to create fibers with nanotopography were made using a base solution containing 240 mg poly-L-lactic acid (PLLA) in 3 g of chloroform. Fifty microliters of one of the following nonsolvents (Table 1) was added to the base solution:

Table 1. Properties of Nonsolvents

nonsolvent	boiling point (°C)	chloroform solubility
water	100	0.056 g/100 g
dmso	189	miscible
ethanol	79	miscible

water, dimethyl sulfoxide (DMSO), or ethanol. In the case of water, two different electrospinning solutions were created: one containing 50μL of deionized water, and one containing 10 μL of deionized water. Another base solution was electrospun using the same electrospinning parameters except the relative humidity was increased to 30−33% to determine if the increased humidity generated nanotopography by vapor induced phase separation.[40,42]

2.1.3. Effect of Nonsolvent Concentration on Fiber Topography. After demonstrating the ability to generate surface structures by changing nonsolvents, we investigated the effects of changing nonsolvent concentration. Only DMSO was used for these experiments since DMSO inclusion generated fibers with more distinct

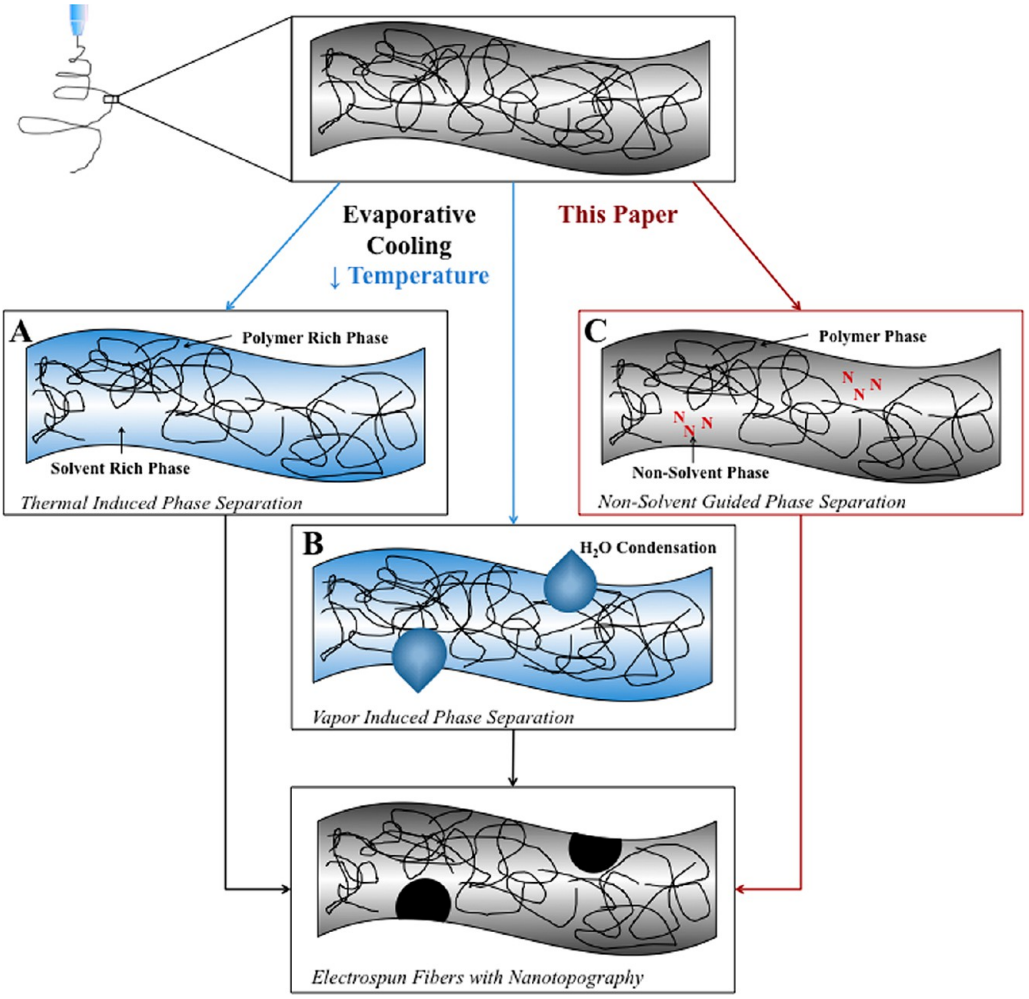

Figure 1. Mechanisms of electrospun fiber surface topography formation. The first mechanism is thermal-induced phase separation (TIPS) (A). With TIPS, rapid evaporation of the solvent cools the fibers and induces a phase separation, resulting in a electrospun fiber surface with surface depressions. The second mechanism is vapor-induced phase separation (VIPS) (B). With VIPS, rapid evaporation cools the fiber and causes water to condense onto the surface of the fiber. Water condensation on the fiber surface creates surface depressions. In this paper, the addition of a nonsolvent to the electrospinning solution induces phase separation (C), giving greater control over the surface topography.

surface nanotopography. Base electrospinning solutions (240 mg of PLLA in 3 g of chloroform) containing varying amounts of DMSO (50−250 μL in 50 μL increments) were electrospun under the same conditions described above. Samples were electrospun in triplicate (n = 3) in that samples were fabricated three times on separate days using freshly prepared electrospinning solutions.

2.1.4. Electrospun Fibers for Cell Culture Experiments. For cell studies, the 100 μL of DMSO in the PLLA/chloroform solution was compared to electrospun fibers containing a smooth surface. The 100 μL of DMSO group was used for cell studies since it contained the largest depressions. To generate fibers with a smooth surface, PLLA was dissolved in 1,1,1,6,6,6-hexafluoro-2-propanol (HFP). Small diameter, smooth surface fibers were generated using 240 mg of PLLA in 3 g of HFP, while large diameter, smooth surface fibers were generated using 240 mg of PLLA in 2 g of HFP. Both solutions were electrospun using the same electrospinning parameters described above (section 2.1.1). Cells were placed on each fiber type where the fibers were fabricated from three separate electrospinning batches (n = 3).

2.2. Scanning Electron Microscopy (SEM). Scanning electron microscopy (SEM) was used to image electrospun fiber samples coated with Pt using a Carl Zeiss Ultra 1540 Dual Beam SEM. Images were captured using a 20 μm aperture and 2 kV accelerating voltage.

2.3. Electrospun Fiber Characterization. *2.3.1. Analysis of Electrospun Fiber Nanotopography, Diameter, and Surface Coverage.* To examine the effects of varying nonsolvent (DMSO) concentration on electrospun fiber surface topography, ImageJ was used to calculate the depression density by counting the number of surface depressions over an area of a fiber. ImageJ was also used to determine the diameter of these depressions along the length of the fiber. Nanotopography was assessed on SEM images from three independently fabricated samples (n > 200 depressions analyzed between three samples).

For electrospun fiber scaffolds used for cell culture, images were analyzed to determine electrospun fiber diameter using a Matlab program previously described.[46] Briefly, images were passed through the radon transform and subsequently differentiated radially. Fiber diameter was then detected by measuring the size of a slope pattern associated with the edges of a fiber. This gave a measurement of the angle of fiber orientation and fiber diameter (n > 50 fibers analyzed from three different samples). To ensure a similar degree of fiber coverage between samples, fiber density was calculated as the number of fibers per mm of sample as previously described.[45] Briefly, a line was drawn perpendicular to the orientation of the fibers, the length of the line was measured in ImageJ, and the number of fibers crossing the line was counted. Fiber density was determined by dividing the number of fibers crossing the line by the distance of the line. An estimation of coverage was made by multiplying the mean diameter of a scaffold by the fiber density to get the diameter density product. The diameter density product is the percentage of the scaffold covered by

fibers if the fibers were perfectly aligned, and a value greater than 100% indicates that the scaffold is completely covered with fibers.

2.3.2. Water Contact Angle Measurements. A goniometer (Rame-Hart 100) was used to make water contact angle measurements using 10 μL of deionized water. The 100 μL DMSO group was selected for the experimental group as it contained the largest nanotopographical depressions. The control groups were the large diameter smooth fibers electrospun using a solution containing 240 mg of PLLA and 2 g of HFP and the small diameter smooth fibers electrospun using a solution containing 240 mg PLLA and 3 g of HFP. Contact angle measurements were performed both parallel and perpendicular to the orientation of fibers on the scaffold. Measurements were performed on three independently fabricated samples for each group (n = 3).

2.4. Cell Culture on Electrospun Fiber Scaffolds. As described in section 2.1.4, three groups were used for cell culture experiments: an electrospun scaffold containing fibers with nanotopographical depressions and electrospun scaffolds containing fibers with smooth topographies but with each scaffold consisting of fibers with distinct fiber diameters. The scaffold with smooth fiber nanotopography and large diameter was selected since it had a similar diameter to the scaffold with fibers containing nanoscale depressions. Additionally, the large and small diameter smooth fibers contained diameters similar to those used in the study by Saino et al.,[25] which demonstrated a diameter dependent response of RAW 264.7 cells to electrospun fibers.

Fibers were not surface treated or coated with any protein before culturing cells. RAW 264.7 cells (ATCC) were cultured in DMEM supplemented with 10% FBS (Invitrogen). 5×10^5 cells were seeded onto three independently fabricated scaffolds for each scaffold topography group and cultured for 24 h in a 12 well culture plate. Electrospun fiber scaffolds with adherent RAW 264.7 cells were then transferred to a new culture plate and new culture media was added with or without 10μg/mL lipopolysaccharide (LPS) (Sigma) as was performed in the study by Saino.[25] Cells were cultured for an additional 24 h before fixation. Cells were then labeled with DAPI nuclei stain, anti-vinculin (1:500, Sigma), and phalloidin (1:700, Sigma) to stain for actin. Three images were taken for each of the three scaffolds in each group (n = 9) using an Olympus DSU. All images were taken at the same exposure and background was removed using the background subtraction function in ImageJ (National Institutes of Health, Bethesda, MD).

2.5. Cell Characterization. *2.5.1. Assessment of Cell Elongation and Cell Adhesion on Electrospun Fiber Scaffolds.* All cell images (n = 9 per electrospinning group) were analyzed to determine the extent of cell elongation using a modified Matlab program similar to previously described procedures.[46] Briefly, the images were passed through the Radon Transform and subsequently differentiated radially. The absolute value of the function was then integrated radially and normalized. The normalized distribution contains information about the orientation of cells in the image, so that a cell with a circular morphology would have no directional orientation. However, a cell that has spread more in one direction than another will have an orientation along the long axis of the cell, and this is detected in the normalized distribution. The distribution was assumed to contain cells with shapes ranging from circles to ovals, so the eccentricity of the normalized distribution was determined.

To perform a cell count, a custom python code was written. Briefly, a k-means algorithm using 5-means was used to threshold the DAPI channel from RAW 264.7 cell images. Then a binary opening operation was performed before counting the number of DAPI objects (cell nuclei) in the image (n = 9 images analyzed per electrospinning group).

2.5.2. Analysis of Cell Metabolism on Electrospun Fiber Scaffolds. To assess the metabolic activity of the macrophages, an MTS assay was performed (CellTiter 96, Promega). Before fixing cells, the macrophage culture media was replaced with fresh culture media supplemented with the MTS agent according to the manufacturer's protocol. Cells were incubated for one hour before supernatant was removed and measured for absorbance at 490 nm. Cell metabolism was assessed on cells cultured on three independently fabricated electrospun fiber samples (n = 3) for each electrospinning group.

2.6. Statistics. Data was analyzed using a one-way ANOVA. When there was statistical significance ($p < 0.05$), a post-hoc Tukey test was performed to determine statistical differences between groups ($p < 0.05$). Data presented in all graphs and text show the mean and standard deviation (mean ± standard deviation).

3. RESULTS AND DISCUSSION

3.1. Electrospun Fiber Nanotopography is Altered by the Inclusion of a Nonsolvent. Our hypothesis that the addition of a nonsolvent to a solution containing PLLA and chloroform would create electrospun fibers with nanotopography was inspired by work from Bognitzki et al.[41] and Megelski et al.[40] Bognitzki et al. proposed that rapid evaporation of dichloromethane cooled the PLLA fibers as they formed, leading to spinodal decomposition of the fiber into polymer rich regions and solvent rich regions (Figure 1A). The solvent rich regions eventually evaporate resulting in depressions on the fiber surface. Megelski et al. called this mechanism thermal induced phase separation (TIPS). The TIPS method was also used to create a theoretical model of porous structure formation in electrospun fibers based on experimental work, further validating TIPS as an appropriate mechanism for surface structure formation on electrospun fibers.[47] Megelski et al. also proposed a second mechanism by which nanotopographical depressions are formed by condensation of water onto the fiber as it forms. This mechanism is called vapor induced phase separation (VIPS, Figure 1B). VIPS proposes that solvent evaporation cools the fiber, causing condensation to form on the fiber surface. With hydrophobic polymers, condensed water on the fiber surface causes a phase separation at the fiber surface to generate regions with water and no polymer. The regions with water become nanoscale depressions on the surface of the electrospun fiber. VIPS was further confirmed in a study by Casper et al.[42] where increasing the relative humidity lead to changes in the size of depressions on electrospun fibers. In addition to water condensation, part of the VIPS mechanism may also depend on the solubility of the primary solvent with water, since water may absorb to the fiber if the solvent is miscible with water.[47,48] Both VIPS and TIPS suggest phase separation as a mechanism for the formation of surface topography. By extension of the phase separation concept, we hypothesized that addition of a nonsolvent (a liquid that does not dissolve the polymer) to the electrospinning solution would induce a phase separation in an electrospun fiber, resulting in a change in the electrospun fiber topography (Figure 1C).

Selection of a control electrospinning solution was critical in testing the nonsolvent hypothesis to ensure that smooth electrospun fibers were produced. Smooth fibers would indicate that the solution was not susceptible to TIPS or VIPS. A control system where electrospun fibers are produced without nanotopography was needed to verify that changes in fiber nanotopography was caused by the addition of the nonsolvent only. The control solution (PLLA/chloroform) was electrospun in a relative humidity condition of less than 28%. Fibers were smooth when produced in environments where the relative humidity was less than 28% through analysis of SEM images (Figure 2A). An additional control was fabricated where the PLLA/chloroform solution was electrospun in an environment where the relative humidity was greater than 33%. The fibers created in the more humid environment did possess nanoscale depressions through analysis of SEM images (Supporting Information SFigure 1). The nanotopography of

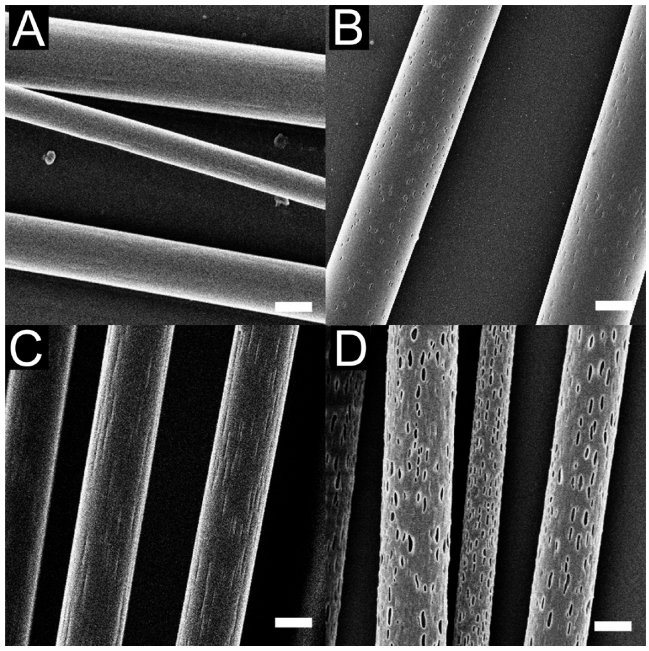

Figure 2. Addition of different nonsolvents changes the surface topography of electrospun fibers. Electrospinning a solution of PLLA/chloroform produces fibers with a smooth topography (A). Addition of 10 μL of deionized water to the PLLA/chloroform electrospinning solution produces fibers with small depressions (B). When 50 μL of ethanol is added to the PLLA/chloroform solution, small and elongated grooves are formed in the fiber (C). Addition of 50 μL of DMSO produces large, distinct depressions in the surface of the fiber (D). All scale bars are 1 μm.

fibers electrospun in higher humidity conditions demonstrated the susceptibility of the PLLA/chloroform solution to VIPS. The drastic change in topography over a small range of relative humidity values was also observed by Megelski et al. (20% relative humidity to 30% relative humidity), although their system consisted of polystyrene dissolved in tetrahydrofuran.[40] The smooth topography generated from a PLLA/chloroform solution when the relative humidity was below 28% made this solution suitable for subsequent testing of our hypothesis. All subsequent electrospinning experiments were performed in a low humidity environment (<28% relative humidity) to eliminate VIPS as a variable when changes in nanotopography were observed.

To test the nonsolvent hypothesis, one of three nonsolvents was added to a solution of PLLA and chloroform: water, ethanol, or DMSO (Table 1). The PLLA/chloroform solution containing 50 μL of deionized water produced poorly formed electrospun fibers (Supporting Information SFigure 2), so another PLLA/chloroform solution containing less deionized water (10 μL) was electrospun. SEM images of fibers produced from the PLLA/chloroform solution containing 10 μL water revealed fibers with nanoscale depressions on the fiber surface (depression length = 92 $\pm$ 17 nm, Figure 2B). In contrast to PLLA/chloroform solutions containing 50 μL of deionized water, PLLA/chloroform solutions containing 50 μL ethanol were capable of forming fibers. SEM images of electrospinning fibers containing ethanol fibers exhibited nanotopographies with shallow, elongated depressions (Figure 2C). Since the longitudinal diameter of the depressions were difficult to discern, the longitudinal diameters were not measured. Finally, PLLA/chloroform solutions containing DMSO generated large depressions with distinct boundaries (Figure 2D). All electrospinning solutions with surface depressions showed an elongated depression boundary, similar to results observed by Bognitzki et al.[41] and Megelski et al..[40] The explanations given by each of these studies is that the depressions become elongated due to the stretching of the fiber. Electrospinning solutions containing DMSO produced fibers with the most distinct change in nanotopography, but the addition of any of the three nonsolvents resulted in changes to the fiber surface compared to the smooth topography generated by the PLLA/chloroform solution alone. The results of these experiments confirmed our hypothesis that addition of a nonsolvent to an electrospinning solution results in a change in fiber nanotopography.

The differences in fiber nanotopography displayed by PLLA/chloroform fibers with different nonsolvent additives is likely the result of two nonsolvent properties (Table 1): (i) the nonsolvent's boiling point and (ii) the nonsolvent's solubility in the primary solvent (i.e. chloroform). The boiling point of water is high compared to the boiling point of chloroform (61.2°C), but water is poorly soluble in chloroform. Due to the poor solubility of water in chloroform, a high concentration of water (50 μL) caused a phase separation between the water and the PLLA/chloroform mixture. The phase separation caused a water phase and a chloroform/PLLA phase to form, preventing a continuous fiber from forming. This explanation is consistent with previous research that observed a high relative humidity generated poorly formed fibers.[30] However, water is soluble in chloroform in small concentrations, so when the concentration of water was small (10 μL) a number of small, stable water/chloroform phases were able to form and resulted in small depressions on the surface of the fiber. In contrast, ethanol has a boiling point (78°C) close to that of chloroform, but unlike water, ethanol is miscible with chloroform. The miscibility of ethanol with chloroform allowed for larger ethanol/chloroform phases to form, explaining the larger grooves in fibers produced with the addition of ethanol compared to the small depressions generated with solutions containing water. The low boiling point of ethanol caused the ethanol to evaporate with the chloroform during the electrospinning process, reducing the size of the ethanol/chloroform phase and consequently the size and depth of the nanoscale depressions. DMSO has the highest boiling point of the nonsolvents tested (189 °C) and is miscible with chloroform. The high boiling point and miscibility with chloroform resulted in a stable DMSO/chloroform phase with little evaporation of the DMSO, ultimately producing the largest and most distinct surface depressions of all nonsolvents tested. Thus, we propose that electrospun fiber surface topography is controllable through the addition of a particular nonsolvent with specific chemical properties (i.e. boiling point and primary solvent solubility). This new method of controlling electrospun fiber nanotopography by addition of a nonsolvent is simple and highly versatile, allowing multiple nonsolvents to be utilized to create distinct surface patterns.

3.2. DMSO Concentration Generates Fibers with Unique Surface Nanotopographies. We then hypothesized that different volumes of nonsolvent would create fibers with distinct patterns of surface nanotopography. More specifically, by adding larger volumes of DMSO to the PLLA/chloroform solution, we hypothesized that electrospun fibers would have larger surface depressions since the volume ratio of nonsolvent/solvent would be greater. Additionally, we also propose fiber diameter may decrease due to an increase in the dielectric

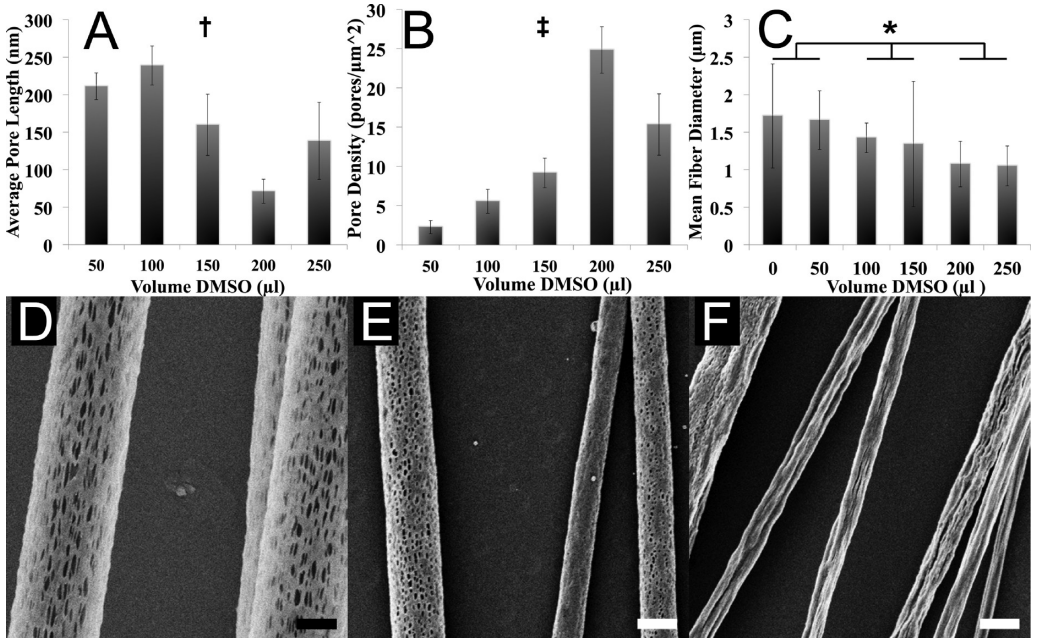

Figure 3. Changing the concentration of nonsolvent alters the topography of electrospun fibers. The changes in depression diameter (A), depression density (B), and fiber diameter (C) were found to change with changes in DMSO concentration. The largest depressions were observed when 100μL (D) of DMSO were used, but increasing the concentration to 200 μL of DMSO (E) decreased the depression diameter and increased the depression density. Increasing the DMSO concentration to a maximum value of 500 μL generated very roughly shaped fibers with few discernable depressions (F). All scale bars are 1μm. † indicates all groups except 150 and 250 μL DMSO groups are significantly different ($p < 0.05$), ‡ indicates all groups are significantly different ($p < 0.05$), * indicates all groups not tied by a flat bar are significantly different (i.e., 0 and 50 μL are not significantly different, $p < 0.05$).

constant of the bulk solution from the addition of DMSO (DMSO ε_r = 46.7, chloroform ε_r = 4.8), since a high dielectric constant is believed to cause a decrease in fiber diameter.[49] Since the first experiment revealed that the addition of DMSO to an electrospinning solution produced fibers with the most distinct depressions, DMSO was studied instead of ethanol or water.

Evaluation of depression diameter (Figure 3A) and density (Figure 3B) revealed a nonlinear response to DMSO concentration. Additionally, there was a trending decrease in fiber diameter (Figure 3C) with increasing DMSO concentration. However, the decrease in fiber diameter may be caused by dilution of the polymer in the electrospinning solution since the addition of nonsolvent effectively reduced the weight percent of the polymer in the total solution. From analysis of the SEM images, there were two critical features worth noting: a maximum depression diameter was observed when 100 μL of DMSO was used (Figure 3D), and a minimum depression diameter was observed when 200 μL of DMSO was used (Figure 3E). Although fibers generated using 200 μL DMSO contained smaller surface depressions, there were significantly more depressions on these fiber than any other group ($p < 0.05$). The fibers fabricated using 250 μL had fewer depressions, and the fibers did not appear to be as cylindrical as the fiber groups with less DMSO. The fibers formed with 500 μL DMSO were even less cylindrically shaped and without the same distinct nanotopographical depressions as the depressions observed at lower concentrations of DMSO (Figure 3F). On the basis of these results characterizing the longitudinal diameter and density of the nanoscale depressions on the surface of the fibers, we confirm our hypothesis that changing nonsolvent concentration alters fiber nanotopography. However, one unexpected result observed from these studies was the correlation between decreasing longitudinal depression diameter with increasing concentrations of DMSO.

The changes in fiber nanotopography observed in the DMSO concentration experiment may be explained by the weight ratio between DMSO to PLLA in the solution. Each solution contained 240 mg of PLLA and 3 g of chloroform before a volume of DMSO was added. The group with the maximum depression diameter (100 μL DMSO) had a DMSO weight (110 mg) that was approximately half of the weight of PLLA in the electrospinning solution (ratio of DMSO to PLLA being 11:24). Fibers generated using 200 μL DMSO (220 mg) contained a nearly equal weight of DMSO in comparison to the PLLA (ratio of DMSO to PLLA being 11:12). When the DMSO weight ($\geq$275 mg)was greater than the weight of PLLA (240 mg), the DMSO was at a high enough concentration to create a large DMSO phase, subsequently forcing the PLLA out of solution. These findings are corroborated by work from Zhang et al. as they observed hollow fibers when a large quantity of the nonsolvent dimethyl formamide (25% of the solution by weight) was added to their electrospinning solution.[50] In the Zhang study, fibers were generated with hollow cores due to the presence of a polymer free dimethyl formamide/dichloromethane phase. The outer polymer shell of the fiber was formed by the PLLA/dichloromethane phase. The near complete separation of PLLA and the dimethyl formamide helps to explain the transition of the fiber surface nanotopography observed in this study where a loss of surface depressions (at 250 μL DMSO) led to inconsistently formed fibers (at 500 μL DMSO) as the nonsolvent concentration increased. This finding explains why many groups that use a nonsolvent to electrospin do not observe the same nanoscale surface features produced here, since it is common to use a high concentration of nonsolvent (1:9 nonsolvent to solvent). Thus,

we propose that addition of nonsolvent up to the weight of polymer in an electrospinning solution will drastically change the surface topography of electrospun fibers.

Although previous studies have investigated other methods to modify electrospun fiber topography including plasma treatment[51] and heavy metal evaporation,[52] the method demonstrated in this study is unique and provides advantages over other methods used in the literature. The main advantage to using the technique presented in this paper is the ease of which electrospun fiber nanotopography can be manipulated without changing surface chemistry, environmental conditions (which can be difficult to control), polymer, or primary solvent. TIPS causes nanoscale depressions to form on electrospun fibers and is believed to be caused by polymer-solvent affinity[44] and the vapor pressure of the solvent.[41] Thus, changing the topography of electrospun fibers using TIPS requires changing the solvent used for electrospinning, which can alter a variety of parameters including fiber diameter.[32] Use of VIPS to generate different nanoscale topographies on electrospun fibers is more attractive than TIPS since the relative humidity can be altered to generate different topographies without changing the polymer or solvent. However, relative humidity can be difficult to control in a narrow range. Additionally, Casper et al. demonstrated in a detailed study on relative humidity (RH) and electrospinning that the changes in electrospun fiber nanotopography due to a change in RH is an increase in the number of depressions while the size of the depressions changes little.[42] The approach presented in this paper to generate electrospun fibers with different nanotopographies does not overcome all of the difficulties listed above (i.e. control of fiber diameter). However, the nonsolvent method presented here should allow different electrospun fiber nanotopographies to be generated using a single polymer/solvent solution with more control of nanotopography variety (i.e. both size and number of depressions) than using relative humidity. Thus, the nonsolvent method of controlling electrospun fiber topography will be instrumental in studying the cell response to electrospun fiber nanotopography, which has not been widely studied.

3.3. Hydrophobicity of Polymer Fibers Unaltered by Nanoscale Depressions. Superhydrophobic structures are typically composed of a hydrophobic material with a nano-structured surface.[53] Typically, a superhydrophobic material has a nano-rough surface that prevents water from sliding along the surface of the material. The inability of a water droplet to slide on a hydrophobic surface with a nanorough surface causes high water contact angles since the droplet is unable to spread out. Thus, we hypothesized that the nanostructured surface of electrospun fibers would be more hydrophobic and create a larger water contact angle than electrospun fibers with a smooth surface.

To test this hypothesis, water contact angle measurements were compared between fibers with nanotopography (fiber diameter = 1.88 ± 0.45 μm, 100 μL DMSO group), a large fiber diameter with a smooth nanotopography (fiber diameter = 1.51 ± 0.446 μm 240 mg of PLLA in 2 g of HFP), and small diameter with a smooth nanotopography (fiber diameter =744 ± 301 nm, 240 mg of PLLA in 3 g of HFP). Since the electrospun scaffolds were collected on a rotating disc, the fibers were highly aligned and thus the scaffold was anisotropic. Therefore, contact angle measurements were made along the length of the fibers (parallel, Figure 4A) and also perpendicular to the direction of the fibers (Figure 4B). No differences in

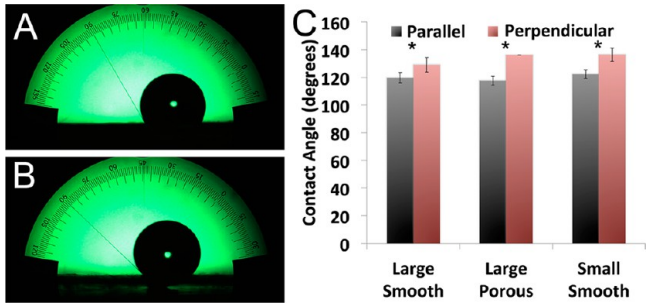

Figure 4. Sessile drop test was used to determine if electrospun fiber topography alters hydrophobicity. Large and small diameter fibers with a smooth topography (large smooth and small smooth, respectively) were compared to fibers with nanoscale depressions (large porous) and similar diameter to the large diameter smooth fiber group. Since the scaffolds were composed of aligned fibers, the contact angle was measured parallel to the fibers (A) and perpendicular to the fibers (B). No differences in contact angle were observed between groups (C), indicating the surface structures did not change the hydrophobicity of the fibers compared to smooth fibers. However, the contact angle parallel to the fibers was lower in all groups compared to the perpendicular water contact angle. * indicates the parallel and perpendicular water contact angles are statistically different ($p < 0.05$).

contact angle measurements were observed between fibers with smooth surfaces, surfaces containing nanoscale depressions, or between scaffolds of different diameter either parallel or perpendicular to the orientation of the fibers (Figure 4C).

However, the water contact angle perpendicular to the direction of the fibers was significantly smaller (less hydrophobic) than the contact angle parallel to the direction of the fibers for fibers with and without surface nanotopography ($p < 0.05$). The similarity of the water contact angle measurements between fibrous scaffolds with and without surface nanotopography led us to reject our hypothesis that a fiber surface with nanotopography would be more hydrophobic (larger water contact angle) than a scaffold consisting of smooth electrospun fibers.

The similarity in water contact angle measurements could be due to the presence of the distinct depressed structures observed on the fibers generated here, rather than a protruding structure typically observed on most hydrophobic surfaces. The protruding structures on a super-hydrophobic surface are believed to reduce the sliding motion of the water droplet.[53] Since the depressed features on our fibers are different than surfaces features containing protrusions, the water droplet may slide more easily. However, the cylindrical surface of the fiber itself reduces the sliding motion of the water droplet perpendicular to the direction of the fibers, causing the contact angle to be larger parallel to the fibers than perpendicular to the fibers. Thus, we conclude that the nonsolvent method of generating nanoscale depressions in electrospun fibers does not alter the hydrophobicity of the electrospun scaffold.

3.4. Nanoscale Depressions Do Not Increase Fiber Degradation Rate. Diffusion of water into the polymer and the rate of bond hydrolysis are the two parameters that define polymer degradation rate.[54] By adding depressions to the fiber surface, the fiber surface area is increased and allows for increased diffusion of water into the fiber. It is possible that fibers with a depressed nanotopography could degrade more quickly than fibers with a smooth surface due to the increase in surface area. Thus, we hypothesized that fibers with a depressed surface structure would degrade more rapidly and thus present

a more significant reduction in fiber diameter in the presence of water than fibers with a smooth topography. Fibers with surface depressions (100 μL DMSO in PLLA/chloroform, 1.88μm $\pm$0.45μm) or fibers with a smooth surface and either a small diameter (744 $\pm$ 301 nm) or a large diameter (1.51 $\pm$ 0.446μm) were incubated in phosphate buffered saline (pH 7.4) for two days. These specific fiber groups and degradation time points were selected to coincide with fiber groups and culture periods used in cell culture experiments. SEM was performed on each fiber group before degradation and after two days of incubation (37 deg C, 5% CO2) of each electrospun fiber group in PBS. A qualitative analysis of SEM images of degraded smooth fibers showed fibers still maintained a smooth surface (Figure 5A and B, small and large diameter

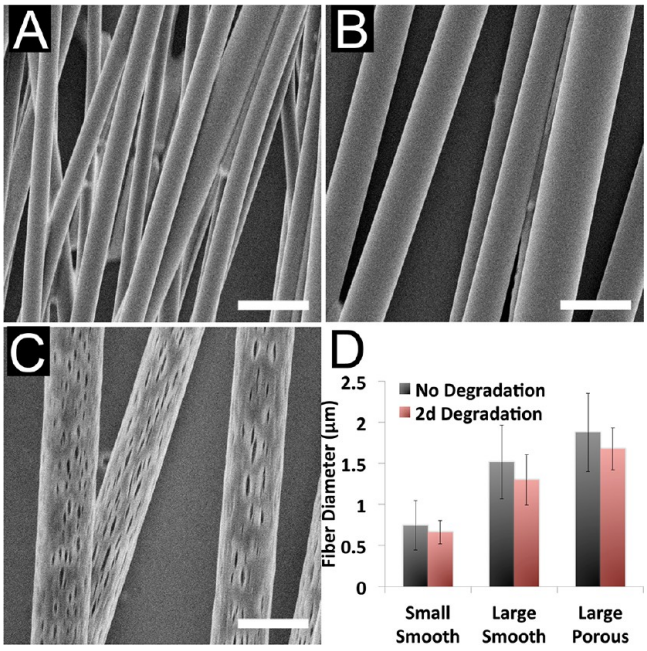

Figure 5. Evaluation of electrospun fiber degradation in PBS over a two-day period. Small diameter smooth fibers (A, small smooth) and large diameter smooth fibers (B, large smooth) show no noticeable changes in fiber diameter or topography after two days of degradation. Similarly, the fibers with nanotopography (C, large porous) show no differences in fiber diameter or topography. A quantitative analysis of fiber diameter shows no significant differences between fiber diameters before and after degradation (D). However, all groups did show an insignificant decrease in fiber diameter over the two-day degradation period. All scale bars are 2 μm.

respectively), and the fibers with depressed nanotopography showed no noticeable reduction in fiber diameter or size of the nanotopographical depressions (Figure 5C). All fibers that were allowed to degrade for two days had smaller diameters, but none of the degraded fiber diameters were significantly different from the starting diameters (Figure 5D). No significant degradation was likely observed due to the high molecular weight of the polymer used (~320 kDa). It is important to note that only fiber diameter was used to quantify fiber degradation since fiber diameter is known to alter cell behavior, as discussed in the introduction. It is possible that there was a significant difference in polymer degradation since polymer weight was not determined, and the decrease in polymer molecular weight could lead to a decrease in fiber mechanical properties. However, we believe the change in PLLA molecular weight is negligible over a two-day period since Dias et al. showed minimal changes in molecular weight of PLLA fibers over a two week period.[55] Since fiber degradation is not influenced by the presence of fiber nanotopography, subsequent changes in cellular behavior observed on fibers with nanotopograhy are likely due to the presence of surface nanotopography and not differences in fiber degradation.

3.5. Cell Extension Along Fibers is Mitigated by Nanoscale Depressions. The effect of electrospun fiber nanotopography on cell behavior was investigated using a macrophage cell line (RAW 264.7 cells). These cells were selected since it is known that macrophages interact with implanted biomaterials including electrospun fibers.[24] Additionally, RAW 264.7 cells are frequently used in cellular experiments to study biological pathways in macrophages and to model cellular processes.[56] Since changes in macrophage (RAW 264.7 cell) morphology have been related to changes in macrophage phenotype,[25,57,58] cell elongation experiments were carried out using the RAW 264.7 macrophage cell line. To simulate an inflammatory phenotype, lipopolysaccharide (LPS) was added to additional cell cultures at a 10μg/mL to determine if cell morphology on electrospun fibers further changed in response to an inflammatory stimulus. LPS is known to increase cell spreading and cause RAW 264.7 cells to adopt a dendritic morphology.[59]

We hypothesized that nanoscale depressions on electrospun fibers would result in less cell spreading when compared to cell spreading on smooth electrospun fibers of similar diameter. This hypothesis is based from observations by Saino et al., who qualitatively demonstrated that electrospun fibers with nanoscale diameters induce less cell spreading.[25] Additionally, a wide variety of cell types have shown less spreading on submicrometer fibers (750 nm or less) compared to fibers with a diameter of greater than a micrometer including fibroblasts,[21,60] neural stem cells,[39] osteoblasts,[37,38] and mesenchymal progenitors.[61] Thus, we propose that cells would respond similarly to nanoscale depressions on the surface of microfibers as they would to fibers with nanoscale diameters.

To test this hypothesis, two smooth fibers conditions were generated each possessing distinct fiber diameters: small diameter smooth (744 $\pm$ 301 nm) and large diameter smooth (1.51 $\pm$ 0.446μm). The diameters of these fibers are similar to those used by Saino et al., where their small diameter fibers (610 $\pm$ 180 nm) produced fewer cytokines than the large diameter fibers (1.6 $\pm$ 0.25μm). Electrospun fibers with nanoscale depressions were generated using the PLLA/chloroform solution using 100 μL DMSO (fiber diameter = 1.88 $\pm$ 0.45μm) since this electrospinning solution produced the largest depressions. The fiber density of all groups were different from each other ($p < 0.05$), with the small diameter fibers having the largest fiber density (1723 $\pm$ 265 fibers/mm) followed by large diameter pitted fibers (667 $\pm$ 53 fibers/mm) and large diameter fibers with a smooth surface (597 $\pm$ 54 fibers/mm). However, if the diameter density product is used to estimate the area covered by the fibers (the product of fiber density and fiber diameter), then only the large diameter smooth fibers had less than 100% of the area covered (90% coverage) while the other groups were completely covered in fibers (diameter density product > 120%). Since all scaffolds were more than 90% covered with electrospun fibers, it is likely that a cell will interact with multiple fibers due to the cells being much larger than the individual fibers.

Cells were labeled for phalloidin (green) to identify cell morphology, vinculin (red) for cell adhesions, and DAPI for cell nuclei. Vinculin was selected as a cell adhesion marker since it is one of the first proteins recruited to a functional cell adhesion.[62] The large diameter smooth fibers allowed for cells to elongate along the length of the fibers (Figure 6A) similar to the results of Saino et al.,[25] and the addition of the inflammatory stimulant LPS did not significantly alter cell elongation (Figure 6B). However, the addition of LPS did increase vinculin labeling compared to cultures without LPS, indicating more cell adhesions were forming in the cultures containing LPS. In contrast to the large diameter smooth fibers, cells cultured on small diameter smooth fibers were more circular in appearance (Figure 6C), and this is in agreement with the results of Saino et al.[25] As with the addition of LPS to cells on large diameter smooth fibers, addition of LPS to cells on small diameter smooth fibers did not significantly change macrophage morphology, but it did increase vinculin labeling (Figure 6D). Cells cultured on electrospun fibers with nanoscale depressions were circular and similar in morphology to cells cultured on the small diameter smooth fibers (Figure 6E), as expected. However, addition of LPS to macrophages on fibers with a nanotopography did not show an increase in vinculin (Figure 5F), unlike either of the fiber groups with a smooth nanotopography. A quantitative analysis of cell elongation confirmed that the large diameter smooth fibers were significantly more elongated than both the small diameter smooth and the fibers with nanotopography ($p<0.05$), but there were no differences in cell elongation on small diameter smooth fibers and fibers with nanoscale depressions (Figure 5G). Since cells on large diameter smooth fibers spread more in the direction of the fibers than any other group, we do not believe that the smaller degree of fiber coverage played a role in cell spreading.

Our results are different from the results obtained by Moroni et al., who found that human mesenchymal stem cells spread more on fibers with nanoscale depressions than those cultured on fibers with a smooth surface.[44] The difference between our results and Moroni's results may be attributed to a difference in cell type, polymer chemistry, or differences in fiber alignment and diameter. An alternative explanation for the cell results on scaffolds with the nanoscale depressions is that the residual DMSO on the fibers may have negatively affected the cells, since DMSO is known to alter the production of inflammatory cytokines in the presence of LPS at low concentrations (≥1% of media volume).[63] However, the samples were sterilized by washing the samples in 70% ethanol, which would remove the DMSO due to DMSO being soluble within ethanol. Even if the ethanol wash did not remove residual DMSO on the fibers with nanoscale depressions, the amount of DMSO would be less than 0.3% of the volume of the culture media. The 0.3% value was calculated based on the number of fibers on the scaffold, and is likely insufficient to cause a change in the cell response based on previous work that showed 0.5% DMSO in solution showed no statistical changes in cytokine production of RAW 264.7 cells.[63] On the basis of this experiment, we confirm our original hypothesis and conclude that a nanoscale fiber structure (fiber diameter or fiber topography) can modify cell spreading. Fibers with a diameter larger than a micrometer normally cause cells to elongate along the length of the fiber, and this observation was made with respect to RAW 264.7 cells both in this study and Saino et al.. However, fibers with a diameter larger than a micrometer and a rough nanotopography

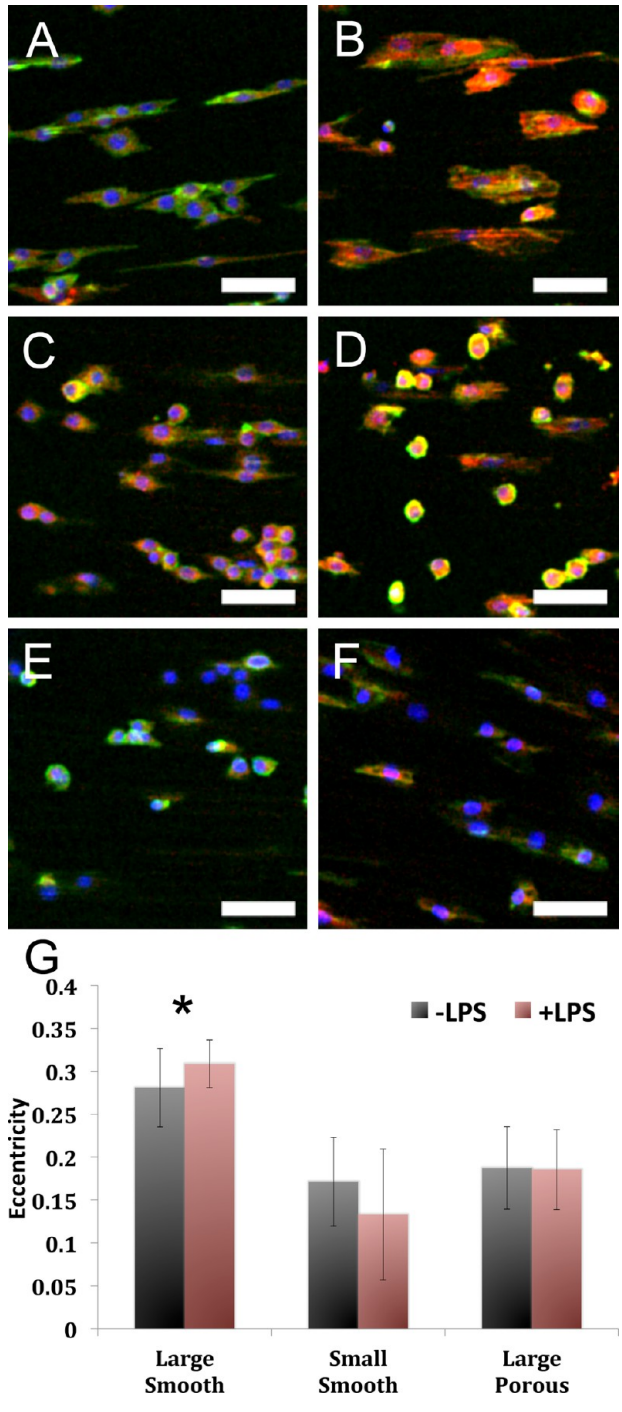

Figure 6. Analysis of macrophage morphology on electrospun fibers with different nanotopographies. Cell morphology was assessed by labeling the cytoskeleton (fibrous actin, green) and cell adhesions (vinculin, red). Cell nuclei were labeled with DAPI (blue). Macrophages (RAW 264.7) were cultured on large diameter smooth fibers (A, large smooth) with the addition of LPS (B) to instigate an inflammatory phenotype. Macrophages were also cultured on small diameter smooth fibers (C, small smooth) with LPS (D) and large diameter fibers with surface depressions (E, large porous) with LPS (F). Only macrophages cultured on large diameter smooth fibers showed an elongated morphology (G) in spite of the fibers with nanotopography having a similar fiber diameter. Unlike the smooth fibers, the fibers with nanotopography appeared to have fewer vinculin markers indicating fewer cell adhesions. Scale bars are 50 μm. *p < 0.05.

cause cells to adopt a round morphology similar to fibers with a submicrometer diameter. This conclusion is important in the context of electrospun fiber scaffolds as tissue engineering scaffolds because the nanotopography of electrospun fibers is rarely considered as a factor in regulating cell behavior.

Although outside the scope of investigation for this paper, one additional explanation for the cell results obtained here may be related to a change in the mechanical properties of the fibers. RAW 264.7 cells are known to adopt a circular morphology on soft hydrogels (tangent modulus = 130 kPa), while RAW 264.7 cells are known to spread more on stiff hydrogels (tangent modulus = 240−840 kPa).[64] For the experiments presented here, if it is assumed that the elastic modulus remains the same for each fiber group, then the smaller cross-sectional area of the fibers with the nanotopographical depressions may be less stiff than the large diameter fibers with a smooth surface, since stiffness is proportional to cross-sectional area. However, if it is the case that the reduced cross-sectional area of the fibers with nanotopographical depressions are not as stiff and explain our current cell results, the same argument could be used to explain the morphology of cells cultured on small diameter fibers. The mechanical properties of the fibers are rarely considered as a factor in regulating cell behavior, but considering the mechanical properties does raise an interesting question not addressed in the literature: do cells behave differently on submicrometer fibers due to the reduced fiber diameter, reduced stiffness, or some combination of both? While this question is outside the scope of this paper, the nonsolvent method of generating fiber nanotopography may aid in answering the question of how fiber stiffness may alter cell behavior since the addition of surface depressions can decrease the cross-sectional area of the fibers.

3.6. Cell Adhesion and Metabolism is Unaltered by Nanotopography Features. The results from the cell morphology experiment showed a reduction in vinculin labeling in cells cultured on electrospun fibers with nanotopography, potentially indicating a reduction in the formation of cell adhesions. Thus, we hypothesized that the reduction in vinculin labeling may be indicative of the number of adherent cells on fibers with nanoscale depressions. However, no differences in the number of cells were observed between electrospun fiber groups (Figure 7A), although all groups without LPS had significantly more cells than groups with LPS ($p < 0.05$). A similar observation was made by Saino et al.,[25] and these results are consistent with biological research involving RAW 264.7 cells where LPS induces apoptosis, thus decreasing the number of adherent cells over time.[65] In addition to performing a cell count, cell metabolism was evaluated using an MTS assay (Figure 7B). However, no differences in metabolism were observed between electrospun fiber groups, although the addition of LPS to cultures revealed an increase in cell metabolism compared to cultures without LPS ($p < 0.05$). On the basis of the results from the metabolism and cell adhesion experiments, we conclude that increased vinculin labeling observed in cells cultured on specific electrospun fibers scaffolds did not correlate to an increase in cell adhesion. This conclusion suggests that electrospun fiber nanotopography can modulate cell elongation without altering the ability of cells to adhere to the scaffold.

Although the study by Moroni and colleagues were the first to demonstrate the ability of electrospun fiber nanotopography to alter cell morphology and metabolism,[44] no additional study has examined cell behavior on fibers with different nanotopography while controlling for other factors, such as fiber diameter. As discussed in the introduction, fiber nanotopography changes according to what solvent or polymer is used as well as the relative humidity of the electrospinning environment. It is difficult to compare cellular results between studies that utilize the same types of cells due to each laboratory using a unique electrospinning solution and electrospinning parameters. Thus, fiber nanotopography could be a hidden variable in cell experiments since there is likely large variability in fiber nanotopography between studies. This is especially true considering the amount of evidence suggesting that the nanoscale structure of a material can cause significant changes in cell behavior (recently reviewed by multiple authors).[66−71] The results of our study affirm the findings of Moroni in that fiber nanotopography alters the ability of a cell to spread. More importantly, we introduce a method of controlling fiber nanotopography and present findings where RAW 264.7 cell spreading is affected by changes in electrospun fiber nanotopography.

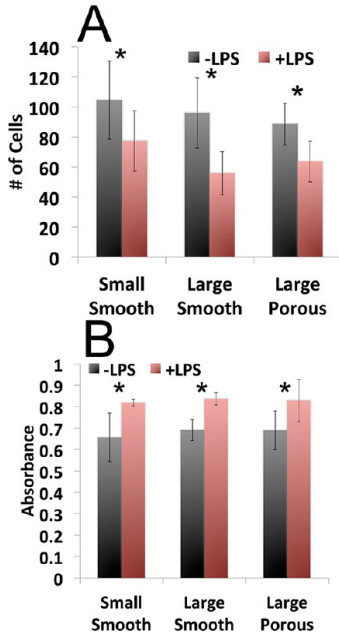

Figure 7. Evaluation of cell adhesion and metabolism on large diameter fibers with a smooth topography (large smooth), small diameter fibers with a smooth topography (small smooth), and fibers with nanotopographical depressions (large porous). The number of adherent cells was determined by counting the number of DAPI labeled nuclei in each image (A). No differences in cell adhesion were observed between groups, except with the addition of LPS. Cell metabolism was assessed using an MTS assay (B), but no differences were observed between groups except with the addition of LPS. The cell adhesion and metabolism data suggest that the topography of electrospun fibers does not prevent macrophage adhesion and viability. *$p < 0.05$ when comparing −LPS to +LPS.

4. CONCLUSIONS

The goal of this work was to establish a method for controlling electrospun fiber surface nanotopography to investigate how fiber nanotopography can alter cell behavior. Adding a nonsolvent into the electrospinning solution created nanoscale despressions on the surface of the fiber. The versatility of the nonsolvent electrospinning method of forming unique surface structures was demonstrated by addition of different non-

solvents or by changing the concentration of a single nonsolvent. Changes in the topography of the electrospun fibers did not alter the hydrophobicity of the electrospun fibers, and the degradation of the fibers was not significantly altered by fibers containing nanoscale depressions. Cells cultured on electrospun fibers with nanotopography were morphologically different compared to cells cultured on smooth fibers with a similar diameter. Although there was a change in cell morphology on fibers with nanotopography, there was no change in cell metabolism or the number of adherent cells. Based on these results, we conclude that our new method of generating electrospun fibers with different surface structures is capable of altering cell spreading without preventing cell adhesion.

■ ASSOCIATED CONTENT

Ⓢ Supporting Information

Fibers generated in humid conditions (relative humidity>33%, SFigure 1) and fibers generated when 50 μL of water was present in the electrospinning solution (SFigure 2). This material is available free of charge via the Internet at http://pubs.acs.org.

■ AUTHOR INFORMATION

Corresponding Author

*E-mail: gilber2@rpi.edu. Phone: (518)-276-2032.

Notes

The authors declare no competing financial interest.

■ ACKNOWLEDGMENTS

The authors would like to thank Dr. Chang Ryu at Rensselaer Polytechnic Institute for the use of his goniometer. This work was supported by NSF CAREER Award 1105125 to R.J.G.

■ REFERENCES

(1) Sill, T. J.; von Recum, H. A. *Biomaterials* **2008**, *29*, 1989−2006.
(2) Lee, Y.-S.; Livingston Arinzeh, T. *Polymers* **2011**, *3*, 413−426.
(3) Shin, S.-H.; Purevdorj, O.; Castano, O.; Planell, J. A.; Kim, H.-W. *J. Tissue Eng.* **2012**, *3*, No. 2041731412443530.
(4) Reneker, D. H.; Yarin, A. L.; Fong, H.; Koombhongse, S. *J. Appl. Phys.* **2000**, *87*, 4531−4547.
(5) Yarin, A. L.; Koombhongse, S.; Reneker, D. H. *J. Appl. Phys.* **2001**, *89*, 3018−3026.
(6) Wang, H. B.; Mullins, M. E.; Cregg, J. M.; Hurtado, A.; Oudega, M.; Trombley, M. T.; Gilbert, R. J. *J. Neural Eng.* **2009**, *6*, No. 016001.
(7) Leach, M. K.; Feng, Z.-Q.; Tuck, S. J.; Corey, J. M. *J. Visualized Exp.* **2011**, No. e2494, DOI: 10.3791/2494.
(8) Kakade, M. V.; Givens, S.; Gardner, K.; Lee, K. H.; Chase, D. B.; Rabolt, J. F. *J. Am. Chem. Soc.* **2007**, *129*, 2777−2782.
(9) Chaurey, V.; Block, F.; Su, Y.-H.; Chiang, P.-C.; Botchwey, E.; Chou, C.-F.; Swami, N. S. *Acta Biomater.* **2012**, *8*, 3982−3990.
(10) Corey, J. M.; Lin, D. Y.; Mycek, K. B.; Chen, Q.; Samuel, S.; Feldman, E. L.; Martin, D. C. *J. Biomed. Mater. Res., Part A* **2007**, *83A*, 636−645.
(11) Leach, M. K.; Feng, Z.-Q.; Gertz, C. C.; Tuck, S. J.; Regan, T. M.; Naim, Y.; Vincent, A. M.; Corey, J. M. *J. Visualized Exp.* **2011**, No. e2389, DOI: 10.3791/2389.
(12) Yang, F.; Murugan, R.; Wang, S.; Ramakrishna, S. *Biomaterials* **2005**, *26*, 2603−2610.
(13) Ghasemi-Mobarakeh, L.; Prabhakaran, M. P.; Morshed, M.; Nasr-Esfahani, M.-H.; Ramakrishna, S. *Biomaterials* **2008**, *29*, 4532−4539.
(14) Yao, L.; O'Brien, N.; Windebank, A.; Pandit, A. *J. Biomed. Mater. Res., Part B* **2009**, *90B*, 483−491.
(15) Lee, J. Y.; Bashur, C. A.; Goldstein, A. S.; Schmidt, C. E. *Biomaterials* **2009**, *30*, 4325−4335.
(16) Liu, X.; Chen, J.; Gilmore, K. J.; Higgins, M. J.; Liu, Y.; Wallace, G. G. *J. Biomed. Mater. Res., Part A* **2010**, *94A*, 1004−1011.
(17) Subramanian, A.; Krishnan, U. M.; Sethuraman, S. *Biomed. Mater.* **2011**, *6*, No. 025004.
(18) Chow, W. N.; Simpson, D. G.; Bigbee, J. W.; Colello, R. J. *Neuron Glia Biol.* **2007**, *3*, 119−126.
(19) Hurtado, A.; Cregg, J. M.; Wang, H. B.; Wendell, D. F.; Oudega, M.; Gilbert, R. J.; McDonald, J. W. *Biomaterials* **2011**, *32*, 6068−6079.
(20) Kim, Y.; Haftel, V. K.; Kumar, S.; Bellamkonda, R. V. *Biomaterials* **2008**, *29*, 3117−3127.
(21) Liu, Y.; Ji, Y.; Ghosh, K.; Clark, R. A. F.; Huang, L.; Rafailovich, M. H. *J. Biomed. Mater. Res., Part A* **2009**, *90A*, 1092−1106.
(22) Johnson, J.; Nowicki, M. O.; Lee, C. H.; Chiocca, E. A.; Viapiano, M. S.; Lawler, S. E.; Lannutti, J. J. *Tissue Eng., Part C* **2009**, *15*, 531−540.
(23) Shang, S.; Yang, F.; Cheng, X.; Walboomers, X. F.; Jansen, J. A. *Eur. Cell. Mater* **2010**, *19*, 180−192.
(24) Cao, H.; Mchugh, K.; Chew, S. Y.; Anderson, J. M. *J. Biomed. Mater. Res., Part A* **2010**, *93A*, 1151−1159.
(25) Saino, E.; Focarete, M. L.; Gualandi, C.; Emanuele, E.; Cornaglia, A. I.; Imbriani, M.; Visai, L. *Biomacromolecules* **2011**, *12*, 1900−1911.
(26) Deitzel, J. .; Kleinmeyer, J.; Harris, D.; Beck Tan, N. . *Polymer* **2001**, *42*, 261−272.
(27) Fridrikh, S. V.; Yu, J. H.; Brenner, M. P.; Rutledge, G. C. *Phys. Rev. Lett.* **2003**, *90*, 144502.
(28) Gupta, P.; Elkins, C.; Long, T. E.; Wilkes, G. L. *Polymer* **2005**, *46*, 4799−4810.
(29) Huang, L.; Bui, N.-N.; Manickam, S. S.; McCutcheon, J. R. *J. Polym. Sci., Part B: Polym. Phys.* **2011**, *49*, 1734−1744.
(30) Vrieze, S. D.; Camp, T. V.; Nelvig, A.; Hagström, B.; Westbroek, P.; Clerck, K. D. *J. Mater. Sci.* **2009**, *44*, 1357−1362.
(31) Lee, S.; Leach, M. K.; Redmond, S. A.; Chong, S. Y. C.; Mellon, S. H.; Tuck, S. J.; Feng, Z.-Q.; Corey, J. M.; Chan, J. R. *Nat. Methods* **2012**, *9*, 917−922.
(32) Wang, H. B.; Mullins, M. E.; Cregg, J. M.; McCarthy, C. W.; Gilbert, R. J. *Acta Biomater.* **2010**, *6*, 2970−2978.
(33) He, L.; Liao, S.; Quan, D.; Ma, K.; Chan, C.; Ramakrishna, S.; Lu, J. *Acta Biomater.* **2010**, *6*, 2960−2969.
(34) Daud, M. F. B.; Pawar, K. C.; Claeyssens, F.; Ryan, A. J.; Haycock, J. W. *Biomaterials* **2012**, *33*, 5901−5913.
(35) Binder, C.; Milleret, V.; Hall, H.; Eberli, D.; Lühmann, T. *J. Biomed. Mater. Res., Part B* **2013**, *101*, 1200−1208.
(36) Qu, J.; Wang, D.; Wang, H.; Dong, Y.; Zhang, F.; Zuo, B.; Zhang, H. *J. Biomed. Mater. Res., Part A* **2013**, *101*, 2667−2678.
(37) Hsu, Y.; Chen, C.; Chiu, J.; Chang, S.; Wang, Y. *J. Biomed. Mater. Res., Part B* **2009**, *91B*, 737−745.
(38) Badami, A. S.; Kreke, M. R.; Thompson, M. S.; Riffle, J. S.; Goldstein, A. S. *Biomaterials* **2006**, *27*, 596−606.
(39) Christopherson, G. T.; Song, H.; Mao, H.-Q. *Biomaterials* **2009**, *30*, 556−564.
(40) Megelski, S.; Stephens, J. S.; Chase, D. B.; Rabolt, J. F. *Macromolecules* **2002**, *35*, 8456−8466.
(41) Bognitzki, M.; Czado, W.; Frese, T.; Schaper, A.; Hellwig, M.; Steinhart, M.; Greiner, A.; Wendorff, J. H. *Adv. Mater.* **2001**, *13*, 70−72.
(42) Casper, C. L.; Stephens, J. S.; Tassi, N. G.; Chase, D. B.; Rabolt, J. F. *Macromolecules* **2003**, *37*, 573−578.
(43) Leong, M. F.; Chian, K. S.; Mhaisalkar, P. S.; Ong, W. F.; Ratner, B. D. *J. Biomed. Mater. Res., Part A* **2009**, *89A*, 1040−1048.
(44) Moroni, L.; Licht, R.; de Boer, J.; de Wijn, J. R.; van Blitterswijk, C. A. *Biomaterials* **2006**, *27*, 4911−4922.
(45) Schaub, N. J.; Gilbert, R. J. *J. Neural Eng.* **2011**, *8*, No. 046026.
(46) Schaub, N. J.; Gilbert, R. J.; Kirkpatrick, S. J. *Proc. SPIE* **2011**, *7897*, 78971D−78971D-5.
(47) Dayal, P.; Liu, J.; Kumar, S.; Kyu, T. *Macromolecules* **2007**, *40*, 7689−7694.

(48) Nezarati, R. M.; Eifert, M. B.; Cosgriff-Hernandez, E. *Tissue Eng., Part C* **2013**, *19*, 810−819.
(49) Guarino, V.; Cirillo, V.; Taddei, P.; Alvarez-Perez, M. A.; Ambrosio, L. *Macromol. Biosci.* **2011**, *11*, 1694−1705.
(50) Zhang, K.; Wang, X.; Jing, D.; Yang, Y.; Zhu, M. *Biomed. Mater.* **2009**, *4*, 035004.
(51) Teraoka, F.; Nakagawa, M.; Hara, M. *Dent. Mater. J.* **2006**, *25*, 560−565.
(52) Shevach, M.; Maoz, B. M.; Feiner, R.; Shapira, A.; Dvir, T. *J. Mater. Chem. B* **2013**, *1*, 5210−5217.
(53) Feng, L.; Li, S.; Li, Y.; Li, H.; Zhang, L.; Zhai, J.; Song, Y.; Liu, B.; Jiang, L.; Zhu, D. *Adv. Mater.* **2002**, *14*, 1857−1860.
(54) Von Burkersroda, F.; Schedl, L.; Göpferich, A. *Biomaterials* **2002**, *23*, 4221−4231.
(55) Dias, J. C.; Ribeiro, C.; Sencadas, V.; Botelho, G.; Ribelles, J. L. G.; Lanceros-Mendez, S. *Polym. Test.* **2012**, *31*, 770−776.
(56) Bordbar, A.; Mo, M. L.; Nakayasu, E. S.; Schrimpe-Rutledge, A. C.; Kim, Y.-M.; Metz, T. O.; Jones, M. B.; Frank, B. C.; Smith, R. D.; Peterson, S. N.; Hyduke, D. R.; Adkins, J. N.; Palsson, B. O. *Mol. Syst. Biol.* **2012**, *8*, 558.
(57) Wójciak-Stothard, B.; Curtis, A.; Monaghan, W.; Macdonald, K.; Wilkinson, C. *Exp. Cell Res.* **1996**, *223*, 426−435.
(58) Lee, H.-S.; Stachelek, S. J.; Tomczyk, N.; Finley, M. J.; Composto, R. J.; Eckmann, D. M. *J. Biomed. Mater. Res., Part A* **2012**, 203−212.
(59) Saxena, R. K.; Vallyathan, V.; Lewis, D. M. *J. Biosci.* **2003**, *28*, 129−134.
(60) Bashur, C. A.; Dahlgren, L. A.; Goldstein, A. S. *Biomaterials* **2006**, *27*, 5681−5688.
(61) Bashur, C. A.; Shaffer, R. D.; Dahlgren, L. A.; Guelcher, S. A.; Goldstein, A. S. *Tissue Eng. Part A* **2009**, *15*, 2435−2445.
(62) Humphries, J. D.; Wang, P.; Streuli, C.; Geiger, B.; Humphries, M. J.; Ballestrem, C. *J. Cell Biol.* **2007**, *179*, 1043−1057.
(63) Xing, L.; Remick, D. G. *J. Immunol.* **2005**, *174*, 6195−6202.
(64) Blakney, A. K.; Swartzlander, M. D.; Bryant, S. J. *J. Biomed. Mater. Res., Part A* **2012**, *100A*, 1375−1386.
(65) Brüne, B.; Gölkel, C.; von Knethen, A. *Biochem. Biophys. Res. Commun.* **1996**, *229*, 396−401.
(66) Kim, D.-H.; Provenzano, P. P.; Smith, C. L.; Levchenko, A. *J. Cell Biol.* **2012**, *197*, 351−360.
(67) Biggs, M. J. P.; Richards, R. G.; Dalby, M. J. *Nanomedicine Nanotechnol. Biol. Med.* **2010**, *6*, 619−633.
(68) McNamara, L. E.; McMurray, R. J.; Biggs, M. J. P.; Kantawong, F.; Oreffo, R. O. C.; Dalby, M. J. *J. Tissue Eng.* **2010**, *1*, 120623.
(69) Guduru, D.; Niepel, M.; Vogel, J.; Groth, T. *Int. J. Artif. Organs* **2011**, *34*, 963−985.
(70) Nava, M. M.; Raimondi, M. T.; Pietrabissa, R. *J. Biomed. Biotechnol.* **2012**, *2012*, 797410.
(71) Anselme, K.; Davidson, P.; Popa, A. M.; Giazzon, M.; Liley, M.; Ploux, L. *Acta Biomater.* **2010**, *6*, 3824−3846.